East Asian Journal on Applied Mathematics
doi: 10.4208/eajam.2024-046.220824

Vol. **16**, No. 1, pp. 72-89
February 2026

# Exact Solutions for a Higher-Order Boussinesq Equation and a New Higher-Order Boussinesq-Like Equation

Wenxia Chen, Weixu Ni*, Yi Wang and Lixin Tian

*Nonlinear Scientific Research Center, Faculty of Science, Jiangsu University, Jiangsu 212013, P.R. China.*

*Received 18 March 2024; Accepted (in revised version) 22 August 2024.*

**Abstract.** A kind of higher-order Boussinesq equation is studied in this work. Based on the Bell polynomials theories, bilinear representations of the equation are derived, and diverse interaction solutions are constructed through Hirota's bilinear method. These include interaction solutions characterized by hyperbolic cosine and cosine functions, as well as interactions between lump and soliton solutions. In addition, generalized bilinear operators are used in order to construct a new higher-order Boussinesq-like equation, while lump and breather solutions are also developed utilizing Hirota's bilinear technique. For the various explicit solutions obtained in this work, several of them are considered to selected particular values for the relevant parameters in order to plot different kind of three-dimensional surfaces with associated two-dimensional density profiles to give a comprehensive understanding of the evolution for various solutions.

**AMS subject classifications**: 65M10, 78A48

**Key words**: Higher-order Boussinesq equation, higher-order Boussinesq-like equation, binary Bell polynomial, Hirota's bilinear method, generalized bilinear method.

## 1. Introduction

In 1834, Russel [21] discovered solitary waves. Since then, soliton theory [5] has attracted increasing attention and has become a significant branch of nonlinear science. The emphasis of the soliton problems is on nonlinear evolution equations (NLEEs) [1,35], many of which are used to describe waves propagation in liquid or gas mixtures [19]. Therefore, exploring the physical meaning of the solutions determined by NLEEs is a crucial problem.

At present, there are various methods to obtain explicit solutions of NLEEs, including the Hirota bilinear representation [8], tanh-coth method [29], Lie symmetry analysis method [12], Darboux transformation [7, 18], Bäcklund transformation [26]. Note that

*Corresponding author. *Email addresses:* chenwx@ujs.edu.cn (W. Chen), nvxmath@163.com (W. Ni), wyy_1998_qsj@163.com (Y. Wang), tianlx@ujs.edu.cn (L. Tian)

 

the Hirota's bilinear method has proven to be the most straightforward and efficient approach for constructing exact solutions for NLEEs. Utilizing different kind of test functions, lumps [27], breathers [32], interaction phenomenon [34] and other explicit solutions could be obtained directly. Moreover, Ma [16,17] introduced a generalized bilinear approach, extending the conventional Hirota bilinear operators. This development led to a new class of bilinear differential equations, employing linear subspaces to construct their solutions.

Among integrable NLEEs, the Boussinesq equation serves as a nonlinear model for shallow water waves. The classical (1+1)-dimensional Boussinesq equation [3] is often expressed as

$$u_{tt} + u_{xx} - 3(u^2)_{xx} - u_{xxxx} = 0, \tag{1.1}$$

the Eq. (1.1), originally proposed by Boussinesq and later derived by Ursell [25] and Whitham [31], has been widely used to model the propagation of long waves in liquid mixtures [10]. Since (1.1) is a completely integrable system, it possesses an infinite number of conservation laws and exhibits Lie group symmetries, as previously established. If the ratio of the $u_{tt}$ term to the $u_{xxxx}$ term is negative, the Eq. (1.1) reduces to the "bad" Boussinesq equation. Conversely, reversing the sign of the $u_{xxxx}$ term yields the "good" Boussinesq equation. The former supports smooth breather and rogue wave solutions, while the latter exhibits singular breather and rogue wave solutions [15].

In recent years, numerous enhanced Boussinesq equations have been developed and investigated. Kuma and Rani [11] obtained the exact solution of the extend (2+1)-dimensional Boussinesq equation employing Lie symmetry method, multiple-soliton solutions of the fourth-order Boussinesq equation are constructed by Wazwaz [30] utilizing Hirota's bilinear method and tanh-coth method. W. Sun and Y. Sun [24] employed the generalized Darboux transformation to derive a degenerate respiration solution of classical Boussinesq equation. In this paper, we consider a higher-order Boussinesq equation (HOBe), viz.

$$\begin{aligned} &u_{tt} + \gamma u_{xx} - \alpha\left(u_{xxxx} + 6u_x^2 + 6uu_{xx}\right) \\ &\quad - \beta\left(15uu_{xxxx} + 30u_xu_{xxx} + 15u_{xx}^2 + 45u^2u_{xx} + 90uu_x^2 + u_{xxxxxx}\right) = 0, \end{aligned} \tag{1.2}$$

where $u = u(x,t), \alpha, \beta, \gamma$ are arbitrary constants. Lump solutions and $N$-soliton solutions of the Eq. (1.2) were derived by Ren [20]. However, to the best our knowledge, the interaction solutions of Eq. (1.2) have not been studied.

It is also worth noting that for some NLEEs, the long-time asymptotics behavior for explicit solutions has an intriguing phenomenon. The investigation is based on Riemann-Hilbert technique and is a popular topic in resent years. Zhiqiang *et al.* [14] constructed a Riemann-Hilbert problem and employed $\overline{\partial}$-steepest descent method to investigate the long-time asymptotics behavior of the explicit solution of the WKI equation with weighted Sobolev initial data. The long-time asymptotics behavior for "good" Boussinesq equation was studied by Charlier *et al.* [4] and others authors, while a defocusing complex modified KdV equation was considered by Riemann-Hilbert approach [28]. Furthermore, utilizing $N$-fold Darboux transformation, the generalized perturbation $(n, N-n)$-fold Darboux transformation is used to solve a two-component nonlinear wave system [33].

Though numerous investigations for Boussinesq equations have been done in few decades, the authors conclude that the interaction solutions of (1.2) have not been investigated so far. This is the main problem studied in the present paper. The objective of this investigation is to establish new interaction solutions of Eq. (1.2), employing the generalized bilinear approach to generate a new Boussinesq-like equation and construct its exact solutions. The Bell polynomials theory proposed by Gilson *et al.* [6], Lambert and Springael [13] is a crucial resource for obtaining the bilinear representation of NLEEs. Furthermore, new research by Singh and Ray [22,23] offers a comprehensive overview based on Bell polynomial approach and Lax pairs. Utilizing close connection between binary Bell polynomials and Hiroa's bilinear operators, the bilinear representation for the Eq. (1.2) can be constructed, while numerous explicit solutions could be developed employing different test functions. By the virtue of generalized Hiroa's bilinear operators extended by Ma [16], one can derive new NLEE systems.

The organization of this paper is as follows. In Section 2, we give a brief introduction to Bell polynomials and Hirota's bilinear operators. In Section 3, a bilinear representation of the Eq. (1.2) is derived and its interaction solutions of (1.2) are constructed. In Section 4, generalized bilinear operators have been used to derive a new Boussinesq-like equation and some of explicit solutions are constructed. Conclusion is given in Section 5.

## 2. Bell Polynomials and Hirota's Bilinear Form

In this section, we introduce Bell polynomials and the Hirota's bilinear form. Assume that $F = F(x_1,\dots,x_l)$ and $G = G(x_1',\dots,x_l')$ are multivariate functions. The classical Hirota's bilinear operators are defined by

$$D_{x_1}^{n_1}\cdots D_{x_l}^{n_l} F\cdot G = \left(\partial_{x_1}-\partial_{x_1'}\right)^{n_1}\cdots\left(\partial_{x_l}-\partial_{x_l'}\right)^{n_l} F(x_1,\dots,x_l) \times G(x_1',\dots,x_l')|_{x_1=x_1',\dots,x_l=x_l'}, \tag{2.1}$$

where $n_1,\dots,n_l$ are arbitrary nonnegative integers [9]. Extending the Hirota bilinear operators, Ma [16, 17] introduced a generalized bilinear method. Let $p\in\mathbb{N}$ be given. The generalized bilinear operators are defined by

$$D_{p,x_1}^{n_1}\cdots D_{p,x_l}^{n_l} F\cdot G = \left(\partial_{x_1}+\eta\partial_{x_1'}\right)^{n_1}\cdots\left(\partial_{x_l}+\eta\partial_{x_l'}\right)^{n_1} F(x_1,\dots,x_l) \times G(x_1',\dots,x_l')|_{x_1=x_1',\dots,x_l=x_l'}, \tag{2.2}$$

and for an integer $l$, the $l$-th power of $\alpha$ is defined by

$$\eta^l = (-1)^{r(l)}, \quad \text{if} \quad l\equiv r(l) \mod p$$

with $0\le r(l)<p$. For example, if $p=3$, then

$$\eta=-1,\quad \eta^2=\eta^3=1,\quad \eta^4=-1,\quad \eta^5=\eta^6=1,\dots,$$

which gives the pattern of symbols

$$-,\ +,\ +,\ -,\ +,\ +,\ \cdots \quad (p=3),$$

for a special case. If $p = 2k$ ($k \in \mathbb{N}$), the generalized Hirota's bilinear operators are reduced to classical Hirota's bilinear operators, since $D_{2k,x} = D_x$.

If $f = f(x_1, x_2, \ldots, x_n)$ is a $C^\infty$ function, then multi-dimensional Bell polynomials ($Y$-polynomials) are defined by

$$Y_{n_1 x_1,\ldots,n_l x_l}(f) \equiv Y_{n_1,\ldots,n_l}(f_{r_1 x_1}, \ldots, f_{r_l x_l}) = e^{-f}\, \partial_{x_1}^{n_1} \cdots \partial_{x_l}^{n_l} e^{f},$$

where $f_{r_1 x_1,\ldots,r_l x_l} = \partial_{x_1}^{r_1} \cdots \partial_{x_l}^{r_l} f$, $0 \le r_i \le n_i$, $0 \le i \le l$ [2].

If $f = f(x, t)$, the multi-dimensional Bell polynomials are converted to two-dimensional Bell polynomials — e.g.

$$\begin{aligned} Y_{x,t}(f) &= f_{x,t} + f_x f_t, \\ Y_{2x,t}(f) &= f_{2x,t} + f_{2x} f_t + 2 f_{x,t} f_x + f_x^2 f_t. \end{aligned}$$

If $f = f(x)$, the multi-dimensional Bell polynomials converted to one-dimensional Bell polynomials — e.g.

$$\begin{aligned} &Y_0(f) = 1, \quad Y_x(f) = f_x, \quad Y_{2x}(f) = f_{2x} + f_x^2, \\ &Y_{3x}(f) = f_{3x} + 3 f_x f_{2x} + f_x^3. \end{aligned}$$

Consider two multivariate functions $v = v(x_1, x_2, \ldots, x_n)$ and $w = w(x_1, x_2, \ldots, x_n)$. The $Y$-polynomials can be generalized to multi-dimensional binary Bell polynomials ($\mathscr{Y}$-polynomials), viz.

$$\begin{aligned} \mathscr{Y}_{n_1 x_1,\ldots,n_l x_l}(v, w) &= Y_{n_1 x_1,\ldots,n_l x_l}(f)\big|_{f_{r_1 x_1,\ldots,r_l x_l}} \\ &= \begin{cases} v_{r_1 x_1,\ldots,r_l x_l}, & r_1 + \cdots + r_l \quad \text{is odd}, \\ w_{r_1 x_1,\ldots,r_l x_l}, & r_1 + \cdots + r_l \quad \text{is even}. \end{cases} \end{aligned} \tag{2.3}$$

The first few lowest order $\mathscr{Y}$-polynomials are

$$\begin{aligned} &\mathscr{Y}_x(v) = v_x, \\ &\mathscr{Y}_{2x}(v, w) = w_{2x} + v_x^2, \\ &\mathscr{Y}_{x,t}(v, w) = w_{x,t} + v_x v_t, \\ &\mathscr{Y}_{3x}(v, w) = v_{3x} + 3 v_x w_{2x} + v_x^2. \end{aligned}$$

Using the functions $v = v(x_1, x_2, \ldots, x_n)$ and $w = w(x_1, x_2, \ldots, x_n)$, we define a new multivariate function $q = w - v$. With $q$ and the constant function 0, we construct $\mathscr{Y}$-polynomials such that the Eq. (2.3) yields the $P$-polynomials

$$P_{n_1 x_1,\ldots,n_l x_l}(q) = \mathscr{Y}_{n_1 x_1,\ldots,n_l x_l}(0, q).$$

It is not difficult to show that $P$-polynomials are $\mathscr{Y}$-polynomials of only even-order. Therefore, the first few lowest order $P$-polynomials can be written without calculations — viz.

$$\begin{aligned} &P_{2x}(q) = q_{2x}, \quad P_{x,t}(q) = q_{xt}, \\ &P_{4x}(q) = q_{4x} + 3 q_{2x}^2, \\ &P_{3x,t}(q) = q_{3x,t} + 3 q_{2x} q_{xt}. \end{aligned}$$

According to [6], the link between $\mathscr{Y}$-polynomials and classical Hirota's bilinear operators can be illustrated by the following identity:

$$\mathscr{Y}_{n_1x_1,\ldots,n_lx_l}(v=\ln F/G, w=\ln FG)=(FG)^{-1}D_{x_1}^{n_1}\cdots D_{x_l}^{n_l}(FG),$$

where $n_1+n_2+\cdots+n_l\geq 1$. In particular, if $F=G$, then the formula (2.3) takes form

$$\begin{aligned}F^{-2}D_{x_1}^{n_1}\cdots D_{x_l}^{n_l}F\cdot F&=\mathscr{Y}_{n_1x_1,\ldots,n_lx_l}(0,q=2\ln F)\\&=\begin{cases}0, & n_1+\cdots+n_l \quad \text{is odd},\\ P_{n_1x_1,\ldots,n_lx_l}(q), & n_1+\cdots+n_l \quad \text{is even}.\end{cases}\end{aligned}\tag{2.4}$$

That is, it is straightforward to obtain the corresponding bilinear equation once a nonlinear evolution equation can be constructed with $P$-polynomials. Some of the lowest order $P$-polynomials provided in this paper may help to simplify computations.

In addition, the binary Bell polynomials $\mathscr{Y}_{n_1x_1,\ldots,n_lx_l}(v,w)$ can be separated into $P$-polynomials and $Y$-polynomials

$$\begin{aligned}(FG)^{-1}D_{x_1}^{n_1}\cdots D_{x_l}^{n_l}(FG)&=\mathscr{Y}_{n_1x_1,\ldots,n_lx_l}(v,w)|_{v=\ln F/G,\ w=\ln FG}\\&=\mathscr{Y}_{n_1x_1,\ldots,n_lx_l}(v,v+q)|_{v=\ln F/G,\ q=2\ln G}\\&=\sum_{n_1+\cdots+n_l \text{ is even}}\sum_{r_1=0}^{n_1}\cdots\sum_{r_l=0}^{n_l}\prod_{i=1}^{l}\binom{n_i}{r_i}P_{r_1x_1,\ldots,r_lx_l}(q)\\&\quad\times Y_{(n_1-r_1)x_1,\ldots,(n_l-r_l)x_l}.\end{aligned}$$

## 3. Exact Solutions of Higher-Order Boussinesq Equations

### 3.1. Hirota's bilinear representation

Considering the higher-order Boussinesq equation (1.2), we employ the following transformation to convert it into the combination of $P$-polynomials:

$$u=h(t)q_{xx},\tag{3.1}$$

where function $h(t)$ will be determined later. Substituting transformation (3.1) into Eq. (1.2) yields

$$\begin{aligned}&h(t)q_{2x,2t}+\gamma h(t)q_{4x}-\alpha\left[h(t)q_{5x}+6h^2(t)q_{3x}^2+6h^2(t)q_{2x}q_{4x}\right]\\&\quad-\beta\Big[15h^2(t)q_{2x}q_{6x}+30h^2(t)q_{3x}q_{5x}+15h^2(t)q_{4x}^2+45h^2(t)q_{4x}\\&\qquad+45h^3(t)q_{2x}^2q_{4x}+90h^3(t)q_{2x}q_{3x}^2+h(t)q_{8x}\Big]=0.\end{aligned}\tag{3.2}$$

Setting $h(t)\equiv 1$, integrating (3.2) twice with respect to $x$, and always selecting the integral constants as 0 yields

$$q_{2t}+\gamma q_{2x}-\alpha\left(q_{3x}+3q_{2x}^2\right)-\beta\left(15q_{2x}q_{4x}+15q_{2x}^3+q_{6x}\right)=0.\tag{3.3}$$

Moreover, the Eq. (3.3) can be written as a combination of $P$-polynomials — viz.

$$P_{2t}(q)+\gamma P_{2x}(q)-\alpha P_{4x}(q)-\beta P_{6x}(q)=0. \tag{3.4}$$

Formula (2.4) is used to transform $P$-polynomials (3.4) into the Hirota's bilinear form

$$\left(D_t^2+\gamma D_z^2-\alpha D_x^4-\beta D_x^6\right) f\cdot f=0. \tag{3.5}$$

According to the definition of classical Hirota's bilinear operators (2.1), the Eq. (3.5) can be expanded as follows:

$$\begin{aligned}&\left(D_t^2+\gamma D_x^2-\alpha D_x^4-\beta D_x^6\right) f\cdot f\\ &=2f_{tt}f-2f_t^2+\gamma\left(2f_{xx}f-2f_x^2\right)-\alpha\left(2f_{xxxx}f-8f_{xxx}f_x+6f_{xx}^2\right)\\ &\quad-\beta\left(2f_{xxxxxx}f-12f_{xxxxx}f_x+30f_{xxxx}f_{xx}-20f_{xxx}^2\right)=0,\end{aligned} \tag{3.6}$$

where $q=2\ln f$, i.e. setting $u=2(\ln f)_{xx}$, we represent the higher-order Boussinesq equation (1.2) as the Hirota bilinear form (3.5).

## 3.2. Interaction solutions employing cosine and hyperbolic cosine

Employing cosine and hyperbolic cosine, we may derive the interaction solution of (1.2), provided that the function $f=f(x,t)$ has the form

$$\begin{aligned}f&=k_1\cosh(g)+k_2\cos(h)+a_7,\\ g&=a_1x+a_2t+a_3,\\ h&=a_4x+a_5t+a_6,\end{aligned} \tag{3.7}$$

where $k_i$, $i=1,2$ and $a_j$, $j=1,2,3,4,5,6,7$ are constants to be determined.

Substituting (3.7) into (3.6), we obtain a set of nonlinear algebraic equations involving $k_i$, $i=1,2$ and $a_j$, $j=1,2,3,4,5,6,7$ by selecting the coefficients of $\cosh(g)$, $\sinh(g)$, $\cos(h)$ and $\sin(h)$ and letting these coefficients to be zero. Solving algebraic equations by Maple, we get two sets of solutions — viz,

**Case 1.**

$$\begin{aligned}&a_1=\varepsilon a_4,\quad a_2=\varepsilon a_4\sqrt{16\beta a_4^4-4\alpha a_4^2-\gamma},\quad a_3=a_3,\quad a_4=a_4,\\ &a_5=\sqrt{16\beta a_4^4-4\alpha a_4^2-\gamma}a_4,\quad a_6=a_6,\quad a_7=0,\quad k_1=k_1,\quad k_2=k_2.\end{aligned} \tag{3.8}$$

To ensure the analyticity of (3.8), we choose $\varepsilon=1$. Substituting (3.8) into (3.7) and employing the transformation $u=2(\ln f)_{xx}$ leads to the interaction solution

$$u(x,t)=\frac{p}{r}-\frac{q}{r^2}, \tag{3.9}$$

where

$$p=-2k_1a_4^2\cosh\left(a_4x+\sqrt{16a_4^4\beta-4a_4^2\alpha-\gamma}a_4t+a_3\right)$$

$$
\begin{aligned}
&-k_2a_4^2\cos\Big(a_4x+\sqrt{16a_4^4\beta-4a_4^2\alpha-\gamma}a_4t+a_6\Big),\\
q=2\Big[&k_1a_4\sinh\Big(a_4x+\sqrt{16a_4^4\beta-4a_4^2\alpha-\gamma}a_4t+a_3\Big)\\
&-k_2a_4\sin\Big(a_4x+\sqrt{16a_4^4\beta-4a_4^2\alpha-\gamma}a_4t+a_6\Big)\Big]^2,\\
r=k_1&\cosh\Big(a_4x+\sqrt{16a_4^4\beta-4a_4^2\alpha-\gamma}a_4t+a_3\Big)\\
&+k_2\cos\Big(a_4x+\sqrt{16a_4^4\beta-4a_4^2\alpha-\gamma}a_4t+a_6\Big).
\end{aligned}
$$

**Case 2.**

$$
\begin{aligned}
&a_1=0,\quad a_2=\sqrt{-\beta a_4^4+\alpha a_4^2+\gamma}a_4,\quad a_3=a_3,\quad a_4=a_4,\quad a_5=0,\\
&a_6=a_6,\quad a_7=0,\quad k_1=\sqrt{-\frac{-16\beta a_4^4+4\alpha a_4^2+\gamma}{\beta a_4^4-\alpha a_4^2-\gamma}}k_2,\quad k_2=k_2,
\end{aligned}
\tag{3.10}
$$

where $a_4,\alpha,\beta,\gamma$ are real numbers that satisfies $\beta a_4^4-\alpha a_4^2-\gamma\neq 0$.

Similarly, substituting expression (3.10) into (3.7) and employing the transformation $u=2(\ln f)_{xx}$, we obtain another interaction solution of the Eq. (1.2), viz.

$$
u(x,t)=-\frac{2k_2a_4^2\cos(a_4x+a_6)}{f}-\frac{2k_2^2a_4^2\sin(a_4x+a_6)^2}{f^2}. \tag{3.11}
$$

Thus, we constructed two different interaction solutions (3.9) and (3.11) based on hyperbolic cosine and cosine. In order to provide a succinct and clear description of the characteristics and capabilities of the interaction phenomenon, we have selected particular values for the relevant parameters mentioned above and they are plotted with the help of Maple software, both two-dimensional and three-dimensional representations were employed to provide a more comprehensive perspective.

For the interaction solution (3.9), we use the parameters $a_3=2,a_6=2,\alpha=2,\beta=1,\gamma=1$, and $a_4=1,5/4,3/2$. Three-dimensional surfaces and associated two-dimensional density profiles of (3.9) are shown in Figs. 1 and 2. We indicate that the Eq. (3.9) can be observed as a set of sharp peaks. When $a_4=1$, the amplitude of the peaks remains stable. However, increasing the value of $a_4$ leads to a rise in amplitude, while the effective area of the Eq. (3.9) decreases as $a_4$ increases.

### 3.3. Lump-soliton solutions

In order to illustrate the interaction of the lump and soliton of Eq. (1.2), we assume that the function $f=f(x,t)$ has the following form:

$$
f=g^2+h^2+k\cosh(n)+a_7, \tag{3.12a}
$$

$$
g=a_1x+a_2t+a_3, \tag{3.12b}
$$

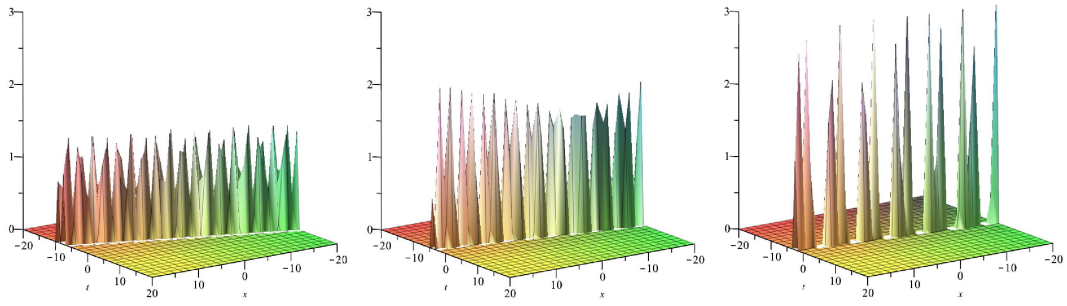

(a) (b) (c)

Figure 1: The interaction solution (3.9) takes $a_3 = 2, a_6 = 2, \alpha = 2, \beta = 1, \gamma = 1$ at (a) $a_4 = 1$, (b) $a_4 = 5/4$, (c) $a_4 = 3/2$.

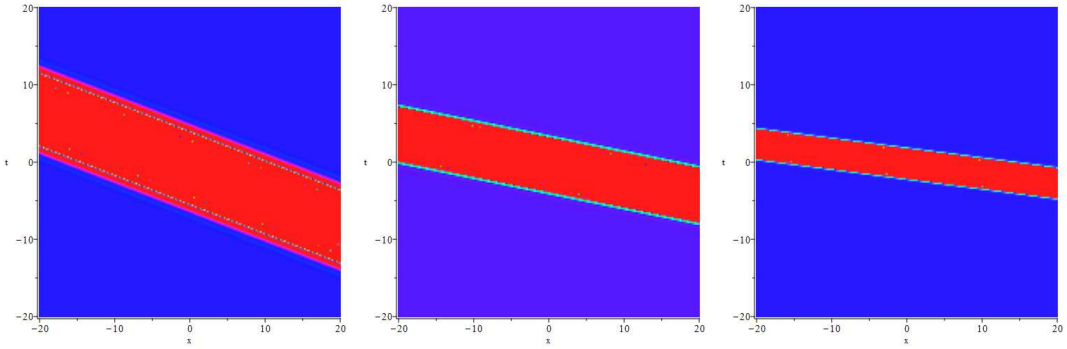

(a) (b) (c)

Figure 2: Associated density profiles of Fig. 1.

$$h = a_4 x + a_5 t + a_6, \tag{3.12c}$$

$$n = k_1 x + k_2 t + k_3, \tag{3.12d}$$

where $k$, $k_i$, $i = 1,2,3$ and $a_j$, $j = 1,2,3,4,5,6,7$ are constants to be determined.

Substituting (3.12) into (3.6), we obtain a set of nonlinear algebraic equations involving $k$, $k_i$, $i = 1,2,3$ and $a_j$, $j = 1,2,3,4,5,6,7$ by selecting all of the coefficients of $x^2, t^2, x, t, xt, \cosh(n), \sinh(n)$ and letting these coefficients to be equal to zero. Solving the algebraic equations by Maple, we obtain two sets of intriguing solutions — viz.

**Case 1.**

$$\begin{aligned} &a_1 = \mathrm{i}a_4, \quad a_2 = \mathrm{i}a_5, \quad a_3 = \mathrm{i}a_6, \quad a_4 = a_4, \quad a_5 = a_5, \quad a_6 = a_6, \quad a_7 = 0, \\ &k = k, \quad k_1 = \frac{\sqrt{2}\sqrt{\beta(-\alpha + \sqrt{\alpha^2 + 4\beta\gamma})}}{4\beta}, \quad k_2 = 0, \quad k_3 = k_3, \end{aligned} \tag{3.13}$$

where $\beta \neq 0$ is a real number and i the imaginary unit. Substituting (3.13) into (3.12), one has

$$f = (\mathrm{i}a_4 x + \mathrm{i}a_5 t + \mathrm{i}a_6)^2 + (a_4 x + a_5 t + a_6)^2$$

$$+k\cosh\left(\frac{\sqrt{2}\sqrt{\beta(-\alpha+\sqrt{\alpha^2+4\beta\gamma})}}{4\beta}x+k_3\right).$$

Using the transformation $u=2(\ln f)_{xx}$, we obtain a lump-soliton solution of the Eq. (1.2), viz.

$$u=\frac{k(-\alpha+\sqrt{\alpha^2+4\beta\gamma})\cosh(k_1x+k_3)}{4\beta f}-\frac{2[kk_1\sinh(k_1x+k_3)]^2}{f^2},\tag{3.14}$$

where

$$k_1=\frac{\sqrt{2}\sqrt{\beta(-\alpha+\sqrt{\alpha^2+4\beta\gamma})}}{4\beta}.$$

**Case 2.**

$$\begin{aligned}&a_1=\mathrm{i}a_4,\quad a_2=\mathrm{i}a_5,\quad a_3=a_3,\quad a_4=a_4,\quad a_5=a_5,\quad a_6=-\mathrm{i}a_3,\\&a_7=0,\quad k=k,\quad k_1=\frac{\sqrt{3}\sqrt{\beta(-\alpha+\sqrt{\alpha^2+3\beta\gamma})}}{3\beta},\quad k_3=k_3,\\&k_2=\sqrt{-\frac{-39\beta\gamma\sqrt{\alpha^2+3\beta\gamma}-40\alpha^2\sqrt{\alpha^2+3\beta\gamma}+99\alpha\beta\gamma+40\alpha^3}{27\beta^2}},\end{aligned}\tag{3.15}$$

where $\beta\neq 0$ is a real number. Substituting expression (3.15) into (3.12), one has

$$f=(\mathrm{i}a_4x+\mathrm{i}a_5t+a_3)^2+(a_4x+a_5t-\mathrm{i}a_3)^2+k\cosh(k_1x+k_2t+k_3).$$

Using the transformation $u=2(\ln f)_{xx}$, we obtain another lump-soliton solution of the Eq. (1.2), viz.

$$u=\frac{2kk_1^2\cosh(k_1x+k_2t+k_3)}{f}-\frac{2(kk_1\sinh(k_1x+k_2t+k_3))^2}{f^2},\tag{3.16}$$

where

$$\begin{aligned}&k_1=\frac{\sqrt{3}\sqrt{\beta(-\alpha+\sqrt{\alpha^2+3\beta\gamma})}}{3\beta},\\&k_2=\sqrt{-\frac{-39\beta\gamma\sqrt{\alpha^2+3\beta\gamma}-40\alpha^2\sqrt{\alpha^2+3\beta\gamma}+99\alpha\beta\gamma+40\alpha^3}{27\beta^2}}.\end{aligned}$$

Similarly, choosing particular values of relevant parameters, we present three-dimensional surfaces and associated two-dimensional density figures of lump-soliton solutions. This helps to have a comprehensive understanding of the interaction of lump and soliton solutions. In this section, we focus on lump-soliton solutions based on Case 1. The sets of parameters in (3.15) are chosen as $a_3=2,a_4=1,a_5=1,k=3,k_3=1,\alpha=1,\beta=2$

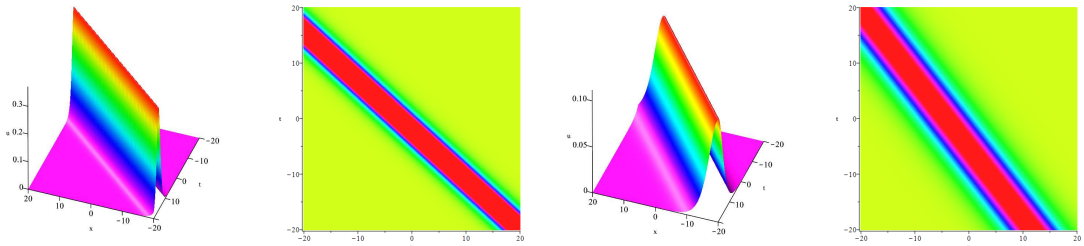

(a) (b) (c) (d)

Figure 3: Interaction solution (3.16) and associated density profiles. (a) $a_3 = 2, a_4 = 1, a_5 = 1, k = 3, k_3 = 1, \alpha = 1, \beta = 2$. (c) $a_3 = 2, a_4 = 4, a_5 = 3, k = 2, k_3 = 1, \alpha = 5, \beta = 2$.

and $a_3 = 2, a_4 = 4, a_5 = 3, k = 2, k_3 = 1, \alpha = 5, \beta = 2$. Three-dimensional surfaces and associated two-dimensional density profiles of Eq. (3.16) are shown in Fig. 3.

There is no doubt that under the constraint of parameters mentioned above, (3.16) demonstrate a typical soliton solutions, the reason for this phenomenon could be explained by the lump was dissolved by the action of retest i while leaving nothing but the soliton solution, could be recognized as a localized wave packet with a positive amplitude that is stable in a non-linear medium.

## 4. Exact Solutions of New Higher-Order Boussinesq-Like Equation

### 4.1. New higher-order Boussinesq-like equation

In this section, we consider a new higher-order Boussinesq-like equation. According to the definition of generalized bilinear operators (2.2), for $p = 3$, for the $D_3$ operator the bilinear representation of the Eq. (1.2) is

$$\left(D_{3,t}^2 + \gamma D_{3,x}^2 - \alpha D_{3,x}^4 - \beta D_{3,x}^6\right) f \cdot f = 0$$

and it can be expanded as

$$\begin{aligned} &\left(D_{3,t}^2 + \gamma D_{3,x}^2 - \alpha D_{3,x}^4 - \beta D_{3,x}^6\right) f \cdot f \\ &= 2f_{tt}f - 2f_t^2 + \gamma\left(2f_{xx}f - 2f_x^2\right) \\ &\quad - 6\alpha f_{xx}^2 - \beta\left(2f_{xxxxxx}f + 20f_{xxx}^2\right) = 0. \end{aligned} \tag{4.1}$$

Using the transformation $u = 2(\ln f)_x$, we obtain a new higher-order Boussinesq-like equation — viz.

$$\begin{aligned} &\int u_{2t}dx + \gamma u_x - \alpha\left(\frac{3}{8}u^4 + \frac{3}{2}u^2u_x + \frac{3}{2}u_x^2\right) \\ &\quad - \beta\left(\frac{11}{32}u^6 + \frac{75}{16}u^4u_x - \frac{135}{8}u^2u_x^2 + 10u_{xx}^2 + u_{5x} + \frac{15}{4}u_x^3 + 3uu_{4x}\right. \\ &\qquad \left. + 5u^3u_{xx} + 30uu_xu_{xx} - \frac{15}{4}u^2u_{xxx} - \frac{15}{2}u_xu_{xxx}\right) = 0. \end{aligned} \tag{4.2}$$

To the best of our knowledge, this equation has not been studied before. The lump solutions and the breather solutions of (4.2) are given in the following sections.

## 4.2. Lump solutions

In order to generate the lump solution of Eq. (4.2), we take the function $f = f(x,t)$ as

$$f = g^2 + h^2 + a_7, \tag{4.3}$$

where

$$g = a_1 x + a_2 t + a_3,$$
$$h = a_4 x + a_5 t + a_6,$$

and the constants $a_j$, $j = 1,2,3,4,5,6,7$ to be determined.

Substituting (4.3) into (4.1), we obtain a set of nonlinear algebraic equations for $a_j$, $j = 1,2,3,4,5,6,7$ by selecting all of the coefficients of $x^2, t^2, x, t, xt$ and letting these coefficients to zero. Solving the algebraic equations Maple, we get the following two sets of solutions.

**Case 1.**

$$\begin{aligned} &a_1 = a_1, \quad a_2 = \sqrt{\gamma} a_4, \quad a_3 = a_3, \quad a_4 = a_4, \\ &a_5 = -\sqrt{\gamma} a_1, \quad a_6 = a_6, \quad a_7 = \frac{3(a_4^2 + a_1^2)\alpha}{\gamma}, \end{aligned} \tag{4.4}$$

where $\gamma \neq 0$ is a real number. Applying the transformation $u = 2(\ln f)_x$ gives the following lump solution of the Eq. (4.2):

$$u = \frac{2(2(a_1 x + \sqrt{\gamma} a_4 t + a_3)a_1 + 2(a_4 x - \sqrt{\gamma} a_1 t + a_6)a_4)}{(a_1 x + \sqrt{\gamma} a_4 t + a_3)^2 + (a_4 x - \sqrt{\gamma} a_1 t + a_6)^2 + 3(a_4^2 + a_1^2)\alpha/\gamma}. \tag{4.5}$$

**Case 2.**

$$\begin{aligned} &a_1 = a_1, \quad a_2 = 0, \quad a_3 = a_3, \quad a_4 = 0, \\ &a_5 = \sqrt{\gamma} a_1, \quad a_6 = a_6, \quad a_7 = \frac{3a_1^2\alpha}{\gamma}, \end{aligned}$$

where $\gamma \neq 0$ is a real number. Applying the transformation $u = 2(\ln f)_x$ leads to another lump solution — viz.

$$u = \frac{4(a_1 x + a_3)a_1}{(a_1 x + a_3)^2 + (\sqrt{\gamma} a_1 t + a_6)^2 + 3a_1^2\alpha/\gamma}. \tag{4.6}$$

For the two lump solutions mentioned above, (4.5) is taken into consideration to plot the three-dimensional surface with associated two-dimensional density profiles in order to investigate the lump solution for the higher-order Boussinesq-like equation (4.2). Specific values of the relevant parameters are selected to illustrate different situations — i.e. set-

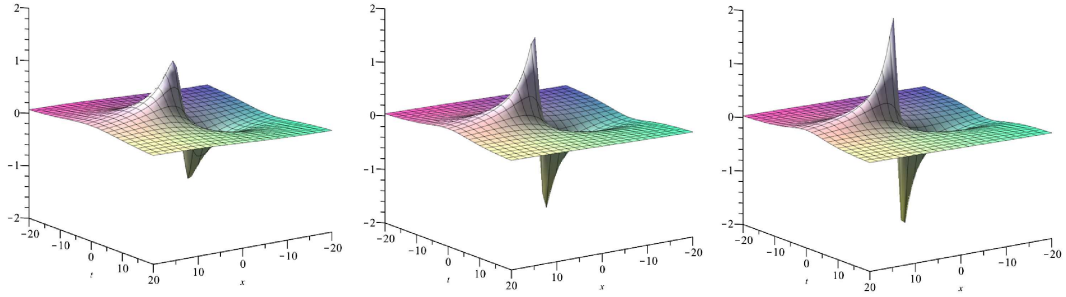

(a) (b) (c)

Figure 4: Lump solutions of (4.5), $a_1 = 6, a_3 = 1, a_4 = 2, a_6 = 1, \alpha = 2$. (a) $\gamma = 2$. (b) $\gamma = 4$. (c) $\gamma = 6$.

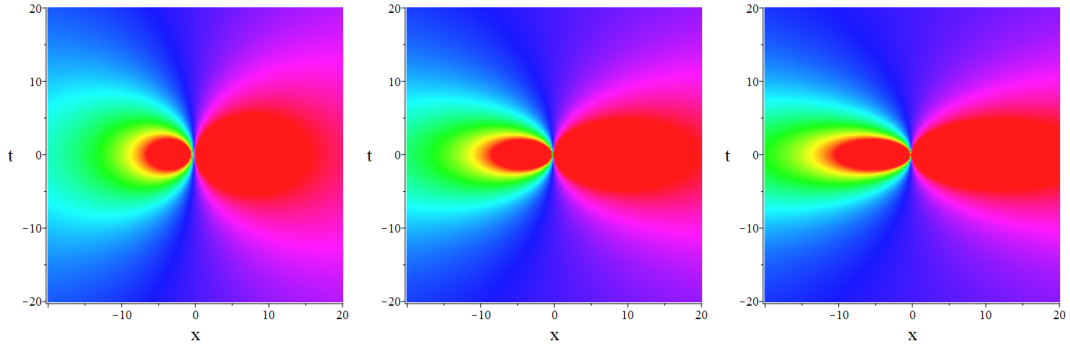


(a) (b) (c)

Figure 5: Associated density profiles of Fig. 4.

ting $a_1 = 6, a_3 = 1, a_4 = 2, a_6 = 1, \alpha = 2$ while $\gamma = 2, 4, 6$ in (4.4). The three-dimensional surface and associated two-dimensional density profiles of Eq. (4.5) are shown in Figs. 4 and 5.

It clearly forms figures that under the constraint of the above parameters, (4.5) demonstrate a typical lump solution form that could be identified as a symmetrical, localized waveform with a peak and a trough. The authors also discovered that the increase of $\gamma$ causes the peak or trough's amplitude to increase and the tip's waveform to sharpen.

The critical points of the lump wave solutions, needed in the consequent analysis, are obtained by solving the following equations:

$$\frac{\partial u(x,t)}{\partial x} = 0, \quad \frac{\partial u(x,t)}{\partial t} = 0.$$

For the lump solution (4.5), the authors found that $u$ attains the maximum and minimum at the points

$$(x_1, t_1) = \left( \frac{-a_1 a_3 \gamma - a_4 a_6 \gamma - \sqrt{3\gamma}\sqrt{\alpha(a_1^2 + a_4^2)^2}}{\gamma(a_1^2 + a_4^2)}, \frac{a_1 a_6 - a_3 a_4}{\sqrt{\gamma}(a_1^2 + a_4^2)} \right),$$

$$(x_2,t_2)=\left(\frac{-a_1a_3\gamma-a_4a_6\gamma+\sqrt{3\gamma}\sqrt{\alpha(a_1^2+a_4^2)^2}}{\gamma(a_1^2+a_4^2)},\frac{a_1a_6-a_3a_4}{\sqrt{\gamma}(a_1^2+a_4^2)}\right),$$

respectively. The critical points are symmetrical with respect to the point

$$(x_0,t_0)=\left(\frac{-a_1a_3\gamma-a_4a_6\gamma}{\gamma(a_1^2+a_4^2)},\frac{a_1a_6-a_3a_4}{\sqrt{\gamma}(a_1^2+a_4^2)}\right).$$

### 4.3. Breather solutions

In order to generate breather solutions of the Eq. (4.2), we take function $f=f(x,t)$ as

$$f=e^{-pg}+b_0\cos(p_1h)+b_1e^{pg} \tag{4.7}$$

with nonzero real numbers $b_0,b_1,p,p_1$, and $g$ and $h$ defined by

$$g=a_1x+a_2t+a_3,$$
$$h=a_4x+a_5t+a_6,$$

where constants $a_j$, $j=1,2,3,4,5,6,7$ to be determined.

Substituting (4.7) into (4.1), we obtain a set of nonlinear algebraic equations for $b_0,b_1$, $p,p_1$ and $a_j$, $j=1,2,3,4,5,6,7$. Selecting all of the coefficients of $e^{-pg},e^{pg}$, $\sin(p_1h)$, $\cos(p_1h)$ and letting these coefficients to be zero. The algebraic equations solved by Maple produce three sets of solutions.

**Case 1.**

$$\begin{aligned}&a_1=0,\quad a_5=0,\quad a_3=a_3,\quad a_6=a_6,\quad b_0=b_0,\quad a_4=\frac{1}{p_1}\sqrt{\frac{3\alpha}{11\beta}},\\&a_2=\frac{\sqrt{33}\sqrt{-9\alpha^3+121\alpha\beta\gamma}}{121p\beta},\quad b_1=\frac{b_0^2(90\alpha^2+121\beta\gamma)}{-36\alpha^2+484\beta\gamma},\end{aligned} \tag{4.8}$$

where $p,p_1,\alpha,\beta,\gamma$ are real numbers such that $p_1\neq0, p\beta\neq0$ and $-36\alpha^2+484\beta\gamma\neq0$. Substituting (4.8) into (4.7), one has

$$f=e^{-pg}+b_0\cos(p_1h)+\frac{b_0^2(90\alpha^2+121\beta\gamma)}{-36\alpha^2+484\beta\gamma}e^{pg},$$

where

$$g=\frac{\sqrt{33}\sqrt{-9\alpha^3+121\alpha\beta\gamma}}{121p\beta}t+a_3,\quad h=\frac{1}{p_1}\sqrt{\frac{3\alpha}{11\beta}}x+a_6.$$

Using of transformation $u=2(\ln f)_x$, we obtain a breather solution of the Eq. (4.2), viz.

$$u=\frac{-(2b_0\sqrt{33}\sqrt{\alpha/\beta}\sin(p_1h))}{11f}. \tag{4.9}$$

**Case 2.**

$$\begin{aligned} a_1 &= \frac{1}{p}\sqrt{-\frac{3\alpha}{11\beta}}, \quad a_2 = 0, \quad a_3 = a_3, \quad a_4 = 0, \quad a_6 = a_6, \quad b_0 = b_0, \\ a_5 &= \frac{\sqrt{33}\sqrt{9\alpha^3 - 121\alpha\beta\gamma}}{121p_1\beta}, \quad b_1 = \frac{b_0^2(-9\alpha^2 + 121\beta\gamma)}{360\alpha^2 + 484\beta\gamma}, \end{aligned} \tag{4.10}$$

where $p, p_1, \alpha, \beta, \gamma$ are real numbers such that $p \neq 0, p_1\beta \neq 0$ and $360\alpha^2 + 484\beta\gamma \neq 0$. Substituting (4.10) into (4.7), one has

$$f = e^{-pg} + b_0\cos(p_1 h) + \frac{b_0^2(-9\alpha^2 + 121\beta\gamma)}{360\alpha^2 + 484\beta\gamma}e^{pg}$$

with

$$g = \frac{1}{p}\sqrt{-\frac{3\alpha}{11\beta}}x + a_3, \quad h = \frac{\sqrt{33}\sqrt{9\alpha^3 - 121\alpha\beta\gamma}}{121p_1\beta}t + a_6.$$

Applying the transformation $u = 2(\ln f)_x$ gives another breather solution of Eq. (4.2), viz.

$$u = \frac{2(b_1\sqrt{33}\sqrt{-\alpha/\beta}e^{pg} - \sqrt{33}\sqrt{-\alpha/\beta}e^{-pg})}{11f}. \tag{4.11}$$

**Case 3.**

$$\begin{aligned} a_1 &= \frac{1}{p}\sqrt{-\frac{3\alpha}{11\beta}}, \quad a_2 = \frac{\sqrt{33\alpha(90\alpha^2 + 121\beta\gamma)}}{121p\beta}, \quad a_3 = a_3, \quad a_4 = \frac{1}{p_1}\sqrt{\frac{3\alpha}{11\beta}}, \\ a_5 &= \frac{\sqrt{33}\sqrt{-90\alpha^3 - 121\alpha\beta\gamma}}{121p_1\beta}, \quad a_6 = a_6, \quad b_0 = b_0, \quad b_1 = b_1, \end{aligned} \tag{4.12}$$

where $p, p_1, \beta$ are real numbers such that $p \neq 0, p_1 \neq 0$ and $\beta \neq 0$. Substituting (4.12) into (4.7), we get

$$f = e^{-pg} + b_0\cos(p_1 h) + b_1 e^{pg}$$

with

$$\begin{aligned} g &= \frac{1}{p}\sqrt{-\frac{3\alpha}{11\beta}}x + \frac{\sqrt{33\alpha(90\alpha^2 + 121\beta\gamma)}}{121p\beta}t + a_3, \\ h &= \frac{1}{p_1}\sqrt{\frac{3\alpha}{11\beta}}x + \frac{\sqrt{33}\sqrt{-90\alpha^3 - 121\alpha\beta\gamma}}{121p_1\beta}t + a_6. \end{aligned}$$

Applying the transformation $u = 2(\ln f)_x$ gives another breather solution of the Eq. (4.2), viz.

$$u = \frac{2(-\sqrt{33}\sqrt{-\alpha/\beta}e^{-pg} - b_0\sqrt{33}\sqrt{\alpha/\beta}\sin(p_1 h) + b_1\sqrt{33}\sqrt{-\alpha/\beta}e^{pg})}{11f}. \tag{4.13}$$

Similarly, specific values for the relevant parameters are selected carefully in order to plotted the three-dimensional surface with associated two-dimensional density and contour figures of breather solutions while (4.9) is taken into consideration in this section, that is, $a_3 = 2, a_6 = 1, b_0 = 2, p = 1, p_1 = 2, \beta = 2, \gamma = 2$ while $\alpha = 2$ and 4, respectively. The three-dimensional surface and associated two-dimensional density and contour profiles of Eq. (4.9) are shown in Figs. 6 and 7.

Eventually, we analyze the evolution of the breather solutions mentioned by comprehending various profiles of (4.9). Seven peaks or troughs with same amplitudes alternate in a straight line across the $(x, t)$ plane. If $\alpha = 2$, the structure is recognized as a common breather. If $\alpha = 4$, the number of peaks or troughs increases (rising from seven to ten) while the amplitudes decrease, we also conclude that the three-dimensional surface of the breather solution (4.9) could be recognized as a collection of several lump solutions — cf. Fig. 4.

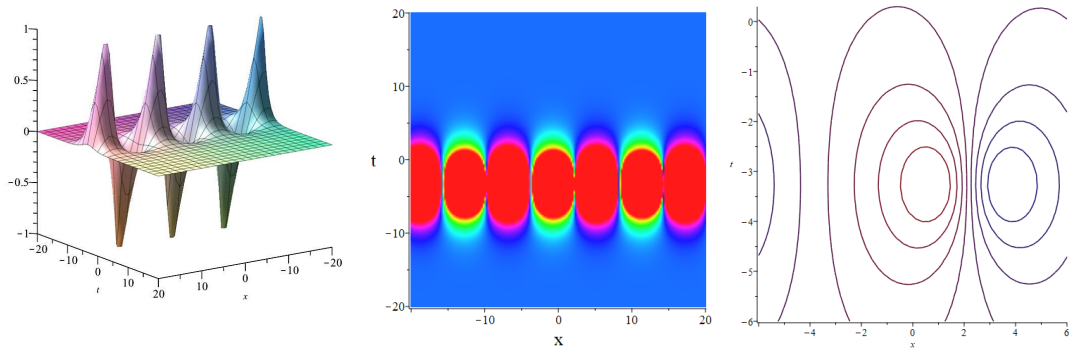


(a) (b) (c)

Figure 6: Breather solution (4.9), associated density profile and contour profile, $a_3 = 2, a_6 = 1, b_0 = 2, p = 1, p_1 = 2, \alpha = 2, \beta = 2, \gamma = 2$.

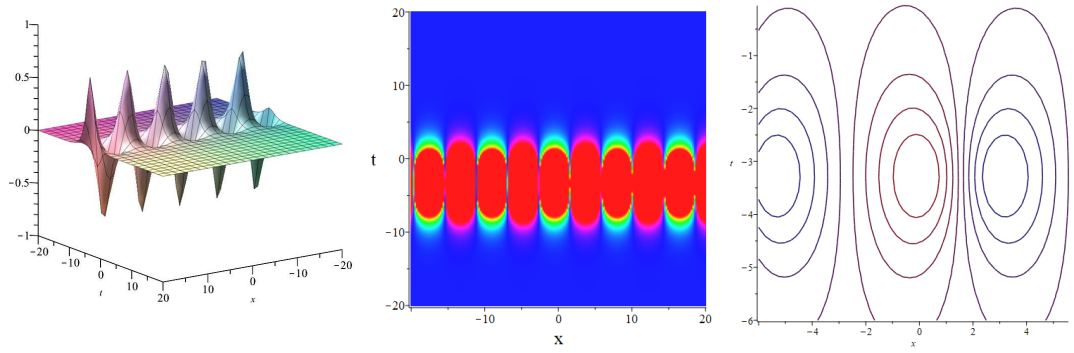


(a) (b) (c)

Figure 7: Breather solution (4.9), associated density profile and contour profile, $a_3 = 2, a_6 = 1, b_0 = 2, p = 1, p_1 = 2, \alpha = 4, \beta = 2, \gamma = 2$.

## 5. Conclusion

In this paper, higher-order Boussinesq equations are investigated by employing Hirota's bilinear technique. Based on the Bell polynomials theory, the Hirota's bilinear representation of Eq. (1.2) is constructed in (3.5). This helps to obtain various explicit solutions and to consider different interaction phenomena.

Utilizing hyperbolic cosine and cosine, two different interaction solutions are shown in (3.9) and (3.11) while (3.9) is considered to plot the three-dimensional surfaces with associated two-dimensional density profiles and a collection of sharp peaks are obtained, displayed in Figs. 1 and 2. Additionally, the interaction phenomenon between lump and soliton is investigated utilizing test function (3.12), two different lump-soliton are given in (3.14) and (3.16), respectively. Accordingly, (3.16) is used to plot different profiles in order to explore the interaction phenomenon, the authors conclude that lump was dissolved by the action of retest "i" so (3.16) could be recognized as a typical soliton, demonstrated in Fig. 3.

Furthermore, utilizing the generate Hirota's bilinear operators performed by Professor Ma with $p = 3$, a new higher-order Boussinesq-like equation is constructed and studied by employing Hirota's bilinear technique. Lump solutions could be identified as a symmetrical, localized waveform with a peak and a trough, two different lumps are obtained in (4.5) and (4.6) while (4.5) is considered to plot the three-dimensional surfaces with associated two-dimensional density profiles, displayed in Figs. 4 and 5. For further analysis, the Eq. (4.5) is used to calculate the critical points. It reaches its maximum value at $(x_1, t_1)$ and its minimum value at $(x_2, t_2)$, respectively. Eventually, three different breather solutions — viz. (4.9), (4.11) and (4.13) are constructed. Additionally, the Eq. (4.9) is used to plot various profiles of the solution. Figs. 6 and 7 illustrate peaks and troughs, recognized as typical form of breather solutions.

Eventually, we have expressed a strong desire to investigate Eq. (1.2) utilizing other technique. Since the Bell polynomials theories are thoroughly introduced in this work, one could try to constructing the bilinear Bäcklund transformation with associated lax pair of Eq. (1.2) which further guarantee the integrability of the system. Once the Lax pair is obtained, one could investigate the long-time asymptotics behavior of the Eq. (1.2) by Riemann-Hilbert approach and Deift-Zhou steepest-descent method. Hope the results of this paper can be used to further study of more general nonlinear differential equations.

## Acknowledgments

This work was supported by the National Natural Science Foundation of China (Grant No. 11731014).

## References

[1] M.J. Ablowitz, D.J. Kaup, A.C. Newell and H. Segur, *Nonlinear evolution equations of physical significance*, Phys. Rev. Lett. **31**, 125–127 (1973).

[2] E.T. Bell, *Exponential polynomials*, Ann. Math. **35**, 258–277 (1934).
[3] J. Boussinesq, *Théorie des ondes et des remous qui se propagent le long d'un canal rectangulaire horizontal, en communiquant au liquide contenu dans ce canal des vitesses sensiblement pareilles de la surface au fond*, J. Math. Pures Appl. **17**, 55–108 (1872).
[4] C. Charlier, J. Lenells and D.S. Wang, *The "good" Boussinesq equation: Long-time asymptotics*, Anal. PDE **16**, 1351–1388 (2023).
[5] N.C. Freeman, *Soliton interactions in two dimensions*, Adv. Appl. Mech. **20**, 1–37 (1980).
[6] C. Gilson, F. Lambert, J. Nimmo and R. Willox, *On the combinatorics of the Hirota D-operators*, Proc. R. Soc. Lond. A Math. Phys. Eng. Sci. **452**, 223–234 (1997).
[7] C.H. Gu, H.S. Hu and Z.X. Zhou, *Darboux Transformations in Integrable Systems: Theory and Their Applications to Geometry*, Springer Science & Business Media (2004).
[8] R. Hirota, *Exact solution of the Korteweg-de Vries equation for multiple collisions of solitons*, Phys. Rev. Lett. **27**, 1192–1194 (1971).
[9] R. Hirota, *The Direct Methods in Soliton Theory*, Cambridge University Press (2004).
[10] P.M. Jordan and C. Feuillade, *On the propagation of harmonic acoustic waves in bubbly liquids*, Int. J. Eng. Sci. **42**, 1119–1128 (2004).
[11] S. Kumar and S. Rani, *Study of exact analytical solutions and various wave profiles of a new extended (2+1)-dimensional Boussinesq equation using symmetry analysis*, J. Ocean Eng. Sci. **7**, 475–484 (2022).
[12] V. Kumar and A. Alqahtani, *Lie symmetry analysis, soliton and numerical solutions of boundary value problem for variable coefficients coupled KdV-Burgers equation*, Nonlinear Dyn. **90**, 2903–2915 (2017).
[13] F. Lambert and J. Springael, *Soliton equations and simple combinatorics*, Acta Appl. Math. **102**, 147–178 (2008).
[14] Z.Q. Li, S.F. Tian and J.J. Yang, *Soliton resolution for the Wadati-Konno-Ichikawa equation with weighted Sobolev initial data*, Ann. Henri Poincaré **23**, 2611–2655 (2022).
[15] Y.K. Liu, B. Li and A.M. Wazwaz, *Novel high-order breathers and rogue waves in the Boussinesq equation via determinants*, Math. Methods Appl. Sci. **43**, 3701–3715 (2020).
[16] W.X. Ma, *Generalized bilinear differential equations*, Stud. Nonlinear Sci. **2**, 140–144 (2011).
[17] W.X. Ma, *Bilinear equations, Bell polynomials and linear superposition principle*, J. Phys.: Conf. Ser. **411**, 012021 (2013).
[18] V.B. Matveev and M.A. Salle, *Darboux Transformations and Solitons*, Springer-Verlag (1991).
[19] G. Morosanu, *Nonlinear Evolution Equations and Applications*, Springer Science & Business Media (1988).
[20] B. Ren, *Painlevé analysis, soliton molecule and lump solution of the higher-order Boussinesq equation*, Adv. Math. Phys. **2021**, 6687632 (2021).
[21] J.S. Russell, *Report on Waves: Made to the Meetings of the British Association in 1842-43*, London (1845).
[22] S. Singh and S.S. Ray, *Newly exploring the Lax pair, bilinear form, bilinear Bäcklund transformation through binary Bell polynomials and analytical solutions for the (2+1)-dimensional generalized Hirota-Satsuma-Ito equation*, Phys. Fluids **35**, 087134 (2023).
[23] S. Singh and S.S. Ray, *Bilinear representation, bilinear Bäcklund transformation, Lax pair and analytical solutions for the fourth-order potential Ito equation describing water waves via Bell polynomials*, J. Math. Anal. Appl. **530**, 127695 (2024).
[24] W.Y. Sun and Y.Y. Sun, *The degenerate breather solutions for the Boussinesq equation*, Appl. Math. Lett. **128**, 107884 (2022).
[25] F. Ursell, *The long-wave paradox in the theory of gravity waves*, Math. Proc. Camb. Philos. Soc. **49**, 685–694 (1953).

[26] H.D. Wahlquist and F.B. Estabrook, *Bäcklund transformation for solutions of the Korteweg-de Vries equation*, Phys. Rev. Lett. **31**, 1386–1390 (1973).
[27] C. Wang, *Spatiotemporal deformation of lump solution to (2+1)-dimensional KdV equation*, Nonlinear Dyn. **84**, 697–702 (2016).
[28] D.S. Wang, L. Xu and Z. Xuan, *The complete classification of solutions to the Riemann problem of the defocusing complex modified KdV equation*, J. Nonlinear Sci. **32**, 3 (2022).
[29] A.M. Wazwaz, *Two reliable methods for solving variants of the KdV equation with compact and noncompact structures*, Chaos, Solitons & Fractals **28**, 454–462 (2006).
[30] A.M. Wazwaz, *Multiple-soliton solutions for the Boussinesq equation*, Appl. Math. Comput. **192**, 479–486 (2007).
[31] G.B. Whitham, *Linear and Nonlinear Waves*, John Wiley & Sons (2011).
[32] G. Xu, A. Gelash, A. Chabchoub, V. Zakharov and B. Kibler, *Breather wave molecules*, Phys. Rev. Lett. **122**, 084101 (2019).
[33] L. Xu, D.S. Wang, X.Y. Wen and Y.L. Jiang, *Exotic localized vector waves in a two-component nonlinear wave system*, J. Nonlinear Sci. **30**, 537–564 (2020).
[34] J.Y. Yang and W.X. Ma, *Abundant interaction solutions of the KP equation*, Nonlinear Dyn. **89**, 1539–1544 (2017).
[35] S.M. Zheng, *Nonlinear Evolution Equations*, Chapman and Hall/CRC (2004).